ARTICLE

Dual-channel recognition of Al^{3+} and Cu^{2+} ions using a chiral pyrene-based fluorescent sensor

Received 00th January 20xx,
Accepted 00th January 20xx

DOI: 10.1039/x0xx00000x

Yuki Matsuura, Masatoshi Asami and Suguru Ito*

A chiral cation sensor comprising two pyrene rings and a diethylene glycol linker has been developed and utilized to detect Al^{3+} and Cu^{2+} ions based on differences in circular dichroism spectra. Remarkably, this sensor afforded the recognition of Al^{3+} and Cu^{2+} ions based on distinct differences in fluorescence spectra. The detection of Al^{3+} ions was achieved based on a typical excimer-to-monomer switching mechanism, whereas the oxidative dimerization of pyrenyl groups was proven to be the origin of the Cu^{2+}-responsive switch in fluorescence spectrum. The Cu^{2+} cation-triggered formation of bipyrene structures, a process that has so far been overlooked in the development of pyrene-based sensors, holds promise for the generation of dual-responsive fluorescent sensors that afford the detection of two different analytes.

Introduction

Molecular sensors that can detect specific metal cations by switching on their photophysical properties have attracted growing interest over the years, owing to the great demand for the detection and visualization of harmful heavy metal ions present in the environment and in living organisms.[1–5] This interest has spurred the development of a considerable number of fluorescent cation sensors comprising various organic fluorophores, such as pyrene,[6,7] fluorescein,[8–10] coumarin,[11–13] and boron-dipyrromethene.[14–16] A clear majority of fluorescent cation sensors rely for their function on the mechanism of the photoinduced electron transfer (PET).[5] The intensity of the sensor's fluorescence can be controlled by switching on or off the PET process in response to the binding of a specific metal cation.

Pyrene-based fluorescent sensors have an advantage over other such sensors in terms of their ability to exhibit both monomer and excimer emission.[7] In fact, in addition to the PET-type sensors, several pyrene-based cation sensors relying on the cation-induced switching between monomer and excimer emission of pyrenyl groups have also been developed. A general structural feature of such sensors is the presence of a linkage between two or more pyrene rings and a cation-recognition moiety, such as a crown ether,[17] a polyether,[18–22] an amide,[23–26] or an amine.[27–30] When the cation-recognition moiety of these sensors captures a specific metal cation, excimer emission is switched on or off as a result of the promotion or prohibition, respectively, of the intramolecular stacking between adjacent pyrenyl groups.

Most organic fluorescent sensors have a single detection mode that shows a one-directional change in the fluorescence spectrum upon the recognition of a suitable cation. Since such cation sensors are only compatible with specific metal ions, the development of dual-channel sensors that can detect two metal ions via different detection modes should be desirable from a practical standpoint.[31–36] However, little is known about dual-channel cation detection afforded by pyrene-based fluorescent sensors.[18,22,37–39] For example, the dynamic excimer emission of a calix[4]crown fluorophore bearing two pyrenyl groups was observed to be switched to a static excimer status or a quenched excimer status in the presence of Cu^{2+} and Pd^{2+} ions, respectively.[38] The combination of off/on and on/off fluorescent switching is another mechanism for dual-channel cation detection afforded by pyrene-based sensors.[39] Although the Cu^{2+} cation-triggered oxidative dimerization of pyrene to produce 1,1′-bipyrene has been reported,[40] this reaction has not been utilized in fluorescent sensors to detect Cu^{2+} ions.

Herein, the dual-channel recognition of Al^{3+} and Cu^{2+} ions has been achieved by using a chiral pyrene-based fluorescent sensor (*S*,*S*)-**1** having a diethylene glycol chain as the cation-recognition site (Fig. 1a). The interaction between the sensor and an Al^{3+} ion was observed to induce the switching from excimer to monomer emission, whereas the oxidative dimerization of pyrenyl groups to produce bipyrene structures was determined to be applicable to the detection of Cu^{2+} ions (Fig. 1b). To the best of our knowledge, the herein-introduced sensor is the first example to elucidate the mechanism of a pyrene-based fluorescent Cu^{2+} detection system that relies for its activity on the oxidative formation of bipyrene structures, which is in sharp contrast to the previous Cu^{2+} sensing systems

Department of Chemistry and Life Science, Graduate School of Engineering Science, Yokohama National University, 79-5 Tokiwadai, Hodogaya-ku, Yokohama 240-8501, Japan. E-mail: suguru-ito@ynu.ac.jp

† Electronic Supplementary Information (ESI) available: [UV, CD, fluorescence, and excitation spectra, determination of association constants, HRMS data, and NMR spectra]. See DOI: 10.1039/x0xx00000x

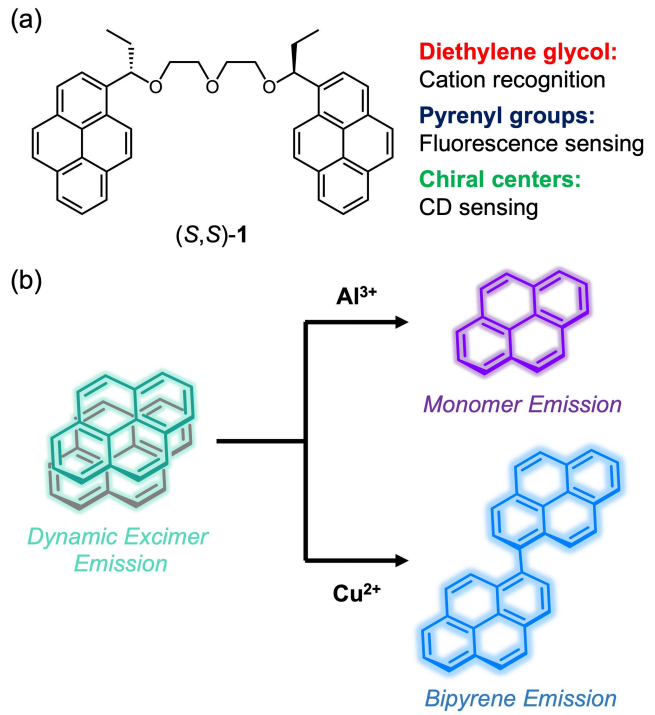

Fig. 1 (a) The chiral pyrene-based fluorescent sensor (*S*,*S*)-**1**. (b) Mechanism of the cation-responsive fluorescence switching process exploited in this work.

based on the fluorescent switching between monomer and excimer or the quenching of fluorescence.

Results and Discussion

Syntheses of (*S*,*S*)-1 and (*S*)-2

The chiral cation receptor (*S*,*S*)-**1,** comprising two pyrenyl groups, and the monopyrenyl compound (*S*)-**2**, utilized as a reference, were synthesized from pyrene-1-carbaldehyde (**3**) (Scheme 1). We have already reported the highly stereoselective synthesis of chiral secondary alcohols achieved via the asymmetric addition of diethylzinc to aldehydes using the *o*-xylylene-type chiral 1,4-amino alcohol **4**[41–44] and the utilization of the thus synthesized compounds in pyrene-based luminescence switching processes.[45,46] By applying this asymmetric reaction to aldehyde **3**, (*S*)-1-(pyren-1-yl)propan-1-ol (**5**) was synthesized (Scheme 1a). Namely, in the presence of the 1,4-amino alcohol (3*R*,7a*S*)-**4**, the reaction between aldehyde **3** and diethylzinc was carried out in toluene/CH_2Cl_2 mixed solvent at room temperature for 18 h. The resulting crude product was purified by column chromatography on silica gel followed by recrystallization from cyclohexane to afford (*S*)-**5** in 67% yield with high enantioselectivity [>99% ee (*S*)]. The reaction of diethylene glycol ditosylate with 2.2 molar amounts of (*S*)-**5** in the presence of NaH (10 mol. amt.) in dry DMF afforded (*S*,*S*)-**1** in 59% yield. Similar to the synthesis of (*S*,*S*)-**1**, the chiral secondary alcohol (*S*)-**5** was treated with NaH (5.0 equiv.) in dry DMF; to the reaction mixture were then added 5.0 equivalents of commercially available 2-bromoethyl ethyl ether to give (*S*)-**2** in 70% yield (Scheme 1b).

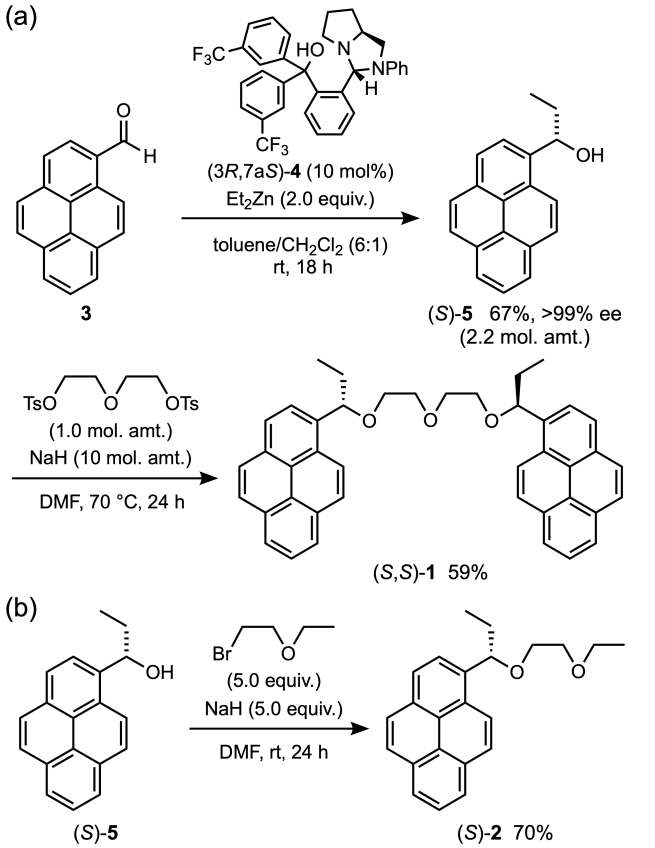

Scheme 1. Enantioselective synthesis of (a) the chiral cation sensor (*S*,*S*)-**1** and (b) the monopyrenyl compound (*S*)-**2**.

UV and CD spectral titration of (*S*,*S*)-1 with cations

When various cations were added to a CH_3CN solution of (*S*,*S*)-**1**, a significant change in its UV absorption spectrum was observed only upon the addition of Cu^{2+} ions (Fig. 2). Specifically, the host compound (*S*,*S*)-**1** in CH_3CN (1.0×10^{-5} M) showed absorption bands at around 276 nm and 343 nm, which should be attributed to the π–π* transitions of the pyrene rings.[47] Perchlorates of a range of cations (i.e., Li^+, NH_4^+, Na^+, Mg^{2+}, Al^{3+}, K^+, Pb^{2+}, and Ba^{2+}) were added to the solution as guest analytes up to a concentration of 1.0×10^{-4} M (10 equiv.). However, no significant changes were observed in the absorption spectra (Fig. 2a). On the other hand, upon the addition of $Cu(ClO_4)_2 \bullet 6H_2O$ to the CH_3CN solution of (*S*,*S*)-**1**, the intensity of the absorption bands at around 276 nm and 343 nm decreased by 22% (Fig. 2b).

The CD spectrum of (*S*,*S*)-**1** in CH_3CN significantly changed after the addition of Al^{3+} ions as well as Cu^{2+} ions (Fig. 3). The CH_3CN solution of the host compound (*S*,*S*)-**1** (1.0×10^{-5} M) showed a negative Cotton effect at around 276 nm and a positive Cotton effect at around 343 nm (Fig. 3a). In addition, the CD spectrum of the enantiomer (*R*,*R*)-**1**, synthesized by the same procedure utilized for the preparation of (*S*,*S*)-**1**, was the mirror image of that of (*S*,*S*)-**1** (Fig. S1). These results exclude the presence of artifacts in the CD spectrum of (*S*,*S*)-**1**. When 10 equivalents of Cu^{2+} cations were added to the solution of (*S*,*S*)-**1**, the Cotton effects were not observed in the resulting solution. Contrary to the small changes observed in the absorption spectrum, the remarkable decrease in the intensity of the CD spectrum should allow the facile detection of target cations. Notably, the disappearance of the Cotton effects was also observed upon the addition of Al^{3+} ions to the CH_3CN solution

of (*S*,*S*)-**1**, although the addition of Al^{3+} ions had not caused any significant change in the absorption spectrum of (*S*,*S*)-**1**. Moreover, the addition of other cations to the CH_3CN solution of (*S*,*S*)-**1** had a negligible impact on the CD spectrum of (*S*,*S*)-**1** (Fig. 3b).

The disappearance of the Cotton effect should be a result of the conformational change of the dipyrenyl derivative (*S*,*S*)-**1** taking place in response to the addition of cations. The absorption bands of the monopyrenyl compound (*S*)-**2** were observed in the same wavelength regions with half intensities as those of (*S*,*S*)-**1** having two pyrenyl groups (Fig. S2). By contrast, the CD spectrum of (*S*)-**2** only showed a negative Cotton effect at around 276 nm (Fig. S3). Accordingly, the positive Cotton effect at around 343 nm observed in the CD spectrum of (*S*,*S*)-**1** should be attributed to the chiral orientation of two pyrene rings controlled by the two asymmetric carbons in the molecule. When Al^{3+} ions were added to the solution of (*S*)-**2**, the Cotton effect at around 276 nm was observed to disappear. Accordingly, the coordination of the ether oxygen to the Al^{3+} ion is assumed to alter the asymmetric environment around the benzylic chiral center.

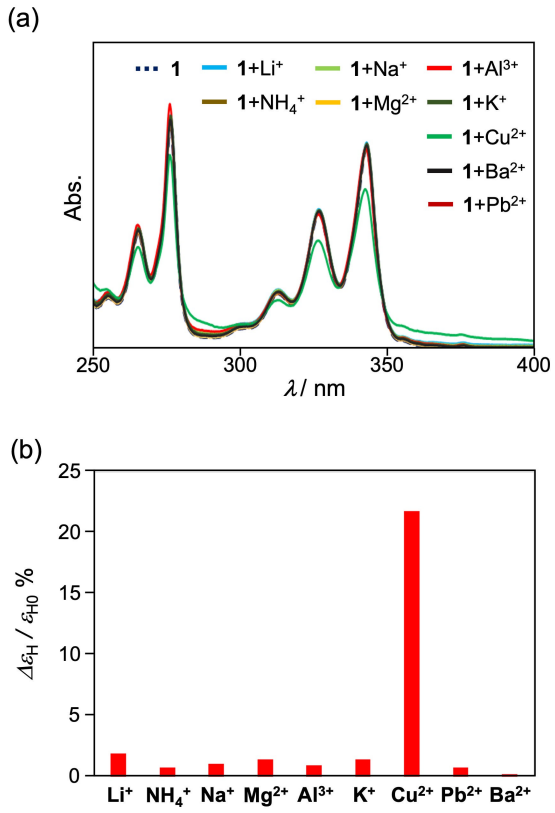

Fig. 2 (a) UV spectra of (*S*,*S*)-**1** in CH_3CN solutions (1.0×10^{-5} M) containing or not containing various cations. (b) Bar graph representing the change in molar extinction coefficient ($\Delta\varepsilon_H/\varepsilon_{H0}$) of (*S*,*S*)-**1** in CH_3CN solutions (1.0×10^{-5} M) at 343 nm resulting from the addition of 10 equivalents of various cations. ε_{H0}: initial molar extinction coefficient of the host compound (*S*,*S*)-**1**. $\Delta\varepsilon_H$: variation of the molar extinction coefficient of (*S*,*S*)-**1** after the addition of the guest analyte.

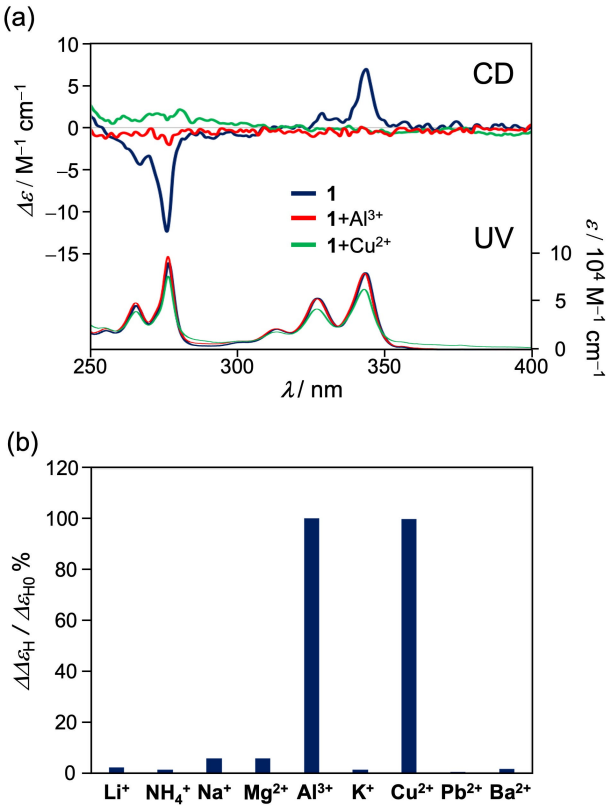

Fig. 3 (a) CD and UV spectra of (*S*,*S*)-**1** in CH_3CN solutions (1.0×10^{-5} M) containing Al^{3+} ions, Cu^{2+} ions, or neither. (b) Bar graph representing the change in molar circular dichroism ($\Delta\Delta\varepsilon_H/\Delta\varepsilon_{H0}$) of (*S*,*S*)-**1** in CH_3CN solutions (1.0×10^{-5} M) at 343 nm resulting from the addition of 10 equivalents of various cations. $\Delta\varepsilon_{H0}$: initial molar circular dichroism of the host compound (*S*,*S*)-**1**. $\Delta\Delta\varepsilon_H$: variation of the molar circular dichroism of (*S*,*S*)-**1** after the addition of the guest analyte.

Fluorescence spectral titration of (*S*,*S*)-1 with cations

The two pyrenyl groups of (*S*,*S*)-**1** showed intramolecular excimer emission in the solution state. In the fluorescence spectrum of a dilute CH_3CN solution (1.0×10^{-5} M) of (*S*,*S*)-**1** (excitation wavelength: 343 nm), a major emission band was observed at 478 nm (Fig. 4a, blue dotted line). Minor emission bands exhibiting vibrational structures were also detected in the 375–400 nm wavelength range. Even at twice the concentration of (*S*,*S*)-**1**, the monopyrenyl compound (*S*)-**2** exhibited a monomer emission with vibrational structures (Fig. S4). This result corroborates the hypothesis that no intermolecular stacks of pyrene rings form in dilute (*S*,*S*)-**1** solutions.

In contrast to the cation-responsive quenching of the CD bands, specific changes were observed in the fluorescence spectrum of (*S*,*S*)-**1** after the addition of Al^{3+} or Cu^{2+} ions to a solution of (*S*,*S*)-**1** (Fig. 4a). When Al^{3+} ions were gradually added to a 5.0×10^{-6} M CH_3CN solution of (*S*,*S*)-**1** up to a final concentration of 10 equivalents, the luminescence color was observed to change from blue-green to violet (Fig. 4b). With a progressive increase in the concentration of the Al^{3+} ion, the intensity of the emission peak at 478 nm decreased, whereas

the intensity of the monomer emission at 377 nm increased (Fig. 4a, red line and Fig. S5). When Cu^{2+} ions were gradually added to the CH_3CN solution of (*S*,*S*)-**1** up to a final concentration of 3 equivalents, the emission color was observed to change from blue-green to bright blue (Fig. 4b). In this case, the intensity of the initial excimer emission also decreased gradually, while the intensities of the emission peaks at around 450 nm as well as at 377 nm increased substantially (Fig. 4a, green line and Fig. S6). A notable decrease in the emission intensity of (*S*,*S*)-**1** was observed in the presence of more than 3 equivalents of Cu^{2+} ions, which should be attributed to the heavy atom effect associated with the presence of Cu^{2+} ions.

Following the addition of Al^{3+} ions, the emission spectrum of (*S*,*S*)-**1** should switch from consisting of a dynamic excimer emission to a monomer emission. Before the addition of cations, the excitation spectrum of (*S*,*S*)-**1** observed at monomer emission (377 nm) was almost identical to that observed at excimer emission (478 nm) (Fig. S7). These spectra showed maximum bands at 275 nm and 342 nm, which are in good agreement with the absorption bands of (*S*,*S*)-**1**. Therefore, the excimer emission of (*S*,*S*)-**1** should be attributed to the dynamic excimer emission caused by the intramolecular interaction between pyrene rings in the excited state.[7] Meanwhile, the formation of the dynamic excimer should be prevented by the interaction between the Al^{3+} ion and the ethylene glycol chain of (*S*,*S*)-**1**, which should account for the observation of monomer emission without changing the excitation spectrum after the addition of 10 equivalents of Al^{3+} ions to the solution of (*S*,*S*)-**1** (Fig. 4c). Since Al^{3+} ions were added as a CH_3CN solution of $Al(ClO_4)_3 \bullet 9H_2O$, a control experiment was carried out by adding 90 equivalents of H_2O to a CH_3CN solution of (*S*,*S*)-**1** (Fig. S8). No significant change in the emission spectrum of (*S*,*S*)-**1** was observed in the presence of H_2O.

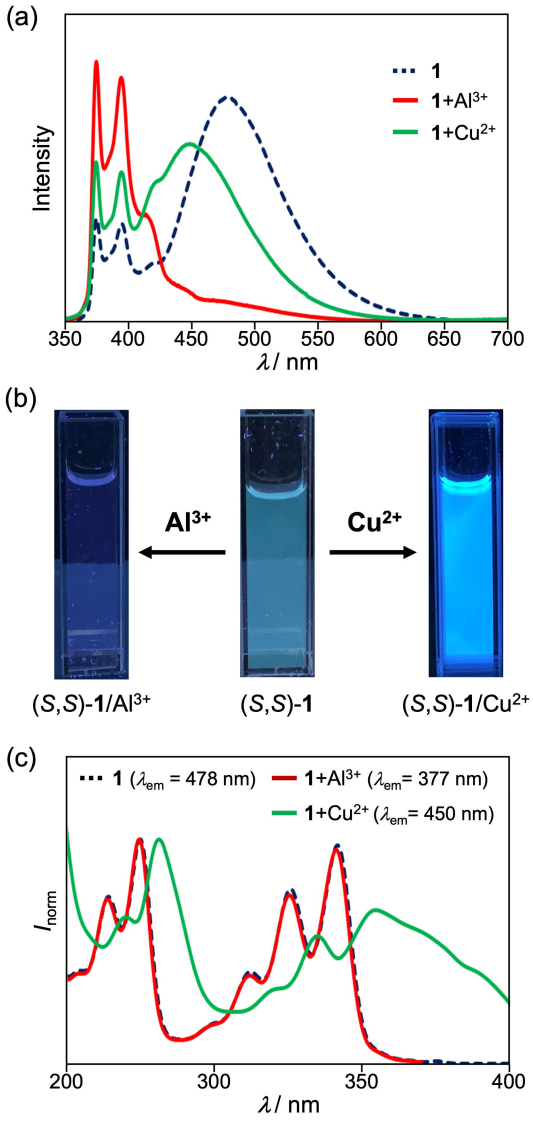

Fig. 4 (a) Fluorescence spectra of (*S*,*S*)-**1**, (*S*,*S*)-**1** with Al^{3+}, and (*S*,*S*)-**1** with Cu^{2+} in CH_3CN ([(*S*,*S*)-**1**]: 5.0 × 10^{-6} M; excitation wavelength: 343 nm). (b) Photographs of (*S*,*S*)-**1**, (*S*,*S*)-**1** with Al^{3+}, and (*S*,*S*)-**1** with Cu^{2+} in CH_3CN ([(*S*,*S*)-**1**]: 5.0 × 10^{-6} M; excitation wavelength: 365 nm). (c) Excitation spectra of (*S*,*S*)-**1**, (*S*,*S*)-**1** with Al^{3+}, and (*S*,*S*)-**1** with Cu^{2+} in CH_3CN ([(*S*,*S*)-**1**]: 5.0 × 10^{-6} M).

The excitation spectrum of (*S*,*S*)-**1** recorded after the addition of Cu^{2+} ions (3 equiv.) indicated that the dynamic excimer emission of (*S*,*S*)-**1** had switched to another type of emission (Fig. 4c). Compared with the excitation spectrum associated with the dynamic excimer emission of (*S*,*S*)-**1**, the excitation spectrum of (*S*,*S*)-**1** recorded in the presence of Cu^{2+} ions was observed in the bathochromic region. Specifically, the excitation spectrum of the emission at 450 nm showed vibrational bands peaking at 281 nm and 355 nm.

The fluorescence band at around 450 nm observed upon the addition of Cu^{2+} ions to the solution of (*S*,*S*)-**1** should be attributed to a bipyrene structure produced by the oxidative dimerization of the pyrenyl groups. When 1.5 molar amounts of $Cu(ClO_4)_2 \bullet 6H_2O$ were added to a CH_3CN solution of (*S*,*S*)-**1** (1.0 × 10^{-4} M), and the resulting solution was stirred at room temperature, the solution's maximum emission wavelength was observed at 455 nm (Fig. S9), as indicated by the results of the titration experiment of the dilute solution (5.0 × 10^{-6} M) of (*S*,*S*)-**1**. Notably, after aqueous workup, the NMR spectrum of the crude product indicated the conversion of (*S*,*S*)-**1** to a complex mixture (Fig. S10). The oxidative dimerization of pyrene in CH_3CN solution triggered by the presence of Cu^{2+} ions has been reported by Nefedov in 2007.[40] Indeed, the ESI-HRMS analysis of the crude mixture indicated the presence of a peak at 588.2664 *m/z* ([(*S*,*S*)-**1**–2H]$^+$, Fig. S11), which is assignable to an intramolecularly cyclized product of (*S*,*S*)-**1** obtained via the oxidative dimerization of the two pyrenyl groups. These results suggest that the addition of Cu^{2+} ions to (*S*,*S*)-**1** solutions promotes the formation of the bipyrene structure to afford macrocyclic compounds and oligomeric mixtures.

1,1′-Bipyrene (**6**) has been reported to show an emission maximum at 432 nm in chloroform solution.[48] When 10 equivalents of Cu^{2+} ions were added to a CH_3CN solution of pyrene (1.0×10^{-5} M), the vibronic fluorescence band resulting from the monomer emission of pyrene was switched to a broad band peaking at 446 nm (Fig. 5a). Pyrene dimer **6** was synthesized separately, and the saturated CH_3CN solution of the isolated **6** showed blue fluorescence at 449 nm (Fig. 5b). Indeed, the fluorescence spectrum of **6** was in good agreement with the emission band at around 450 nm recorded for the solution of (*S*,*S*)-**1** and Cu^{2+} ions (Fig. 5b). These results support the hypothesis that the spectral changes of (*S*,*S*)-**1** triggered by the addition of Cu^{2+} ions are due to the oxidative dimerization of pyrenyl groups.

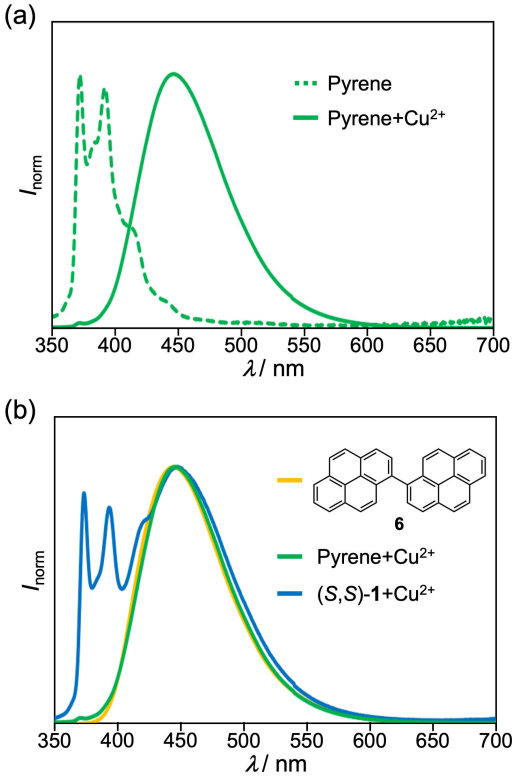

Fig. 5 (a) Fluorescence spectra of pyrene alone and pyrene in the presence of Cu^{2+} recorded in CH_3CN ([pyrene]: 1.0×10^{-5} M; excitation wavelength: 343 nm). (b) Fluorescence spectra of saturated dimer **6** in CH_3CN, pyrene (1.0×10^{-5} M) in the presence of Cu^{2+} in CH_3CN, and (*S*,*S*)-**1** (5.0×10^{-6} M) in the presence of Cu^{2+} in CH_3CN (excitation wavelength: 343 nm).

Conclusions

The chiral pyrene-based sensor (*S*,*S*)-**1** was developed as an efficient dual-channel cation sensor that can recognize Al^{3+} and Cu^{2+} ions. A substantial decrease in the intensity of the absorption spectrum of (*S*,*S*)-**1** was observed only after the addition of Cu^{2+} ions, whereas the CD bands of (*S*,*S*)-**1** were sensitive to the presence of both Al^{3+} and Cu^{2+} ions. Accordingly, the presence of Al^{3+} and Cu^{2+} ions should be distinguished by combining the UV and CD methods. Moreover, (*S*,*S*)-**1** was capable of selectively recognizing Al^{3+} and Cu^{2+} ions based on the different responses of the fluorescence spectrum. The detection of Al^{3+} ions was based on the fluorescence signal switching between the emission of a dynamic excimer of pyrene rings and that of a pyrene ring monomer. Meanwhile, the fluorescence spectral change occurring upon the addition of Cu^{2+} ions to the solution of (*S*,*S*)-**1** was attributed to the oxidative dimerization of the pyrenyl groups. The results of this study indicate for the first time that the fluorescence detection of Cu^{2+} ions can be achieved via the formation of the bipyrene structure. These findings should be applicable to the creation of new dual-channel sensors that are able to specifically recognize a range of metal cations.

Experimental

Instrumentation and Materials.

All air-sensitive experiments were carried out under an atmosphere of argon unless otherwise noted. FTIR spectra were recorded on a JASCO FT/IR 6200 spectrometer. ^1H and ^{13}C NMR spectra were recorded on a Bruker DRX-500 and an ECA-500 spectrometers using tetramethylsilane as an internal standard. Optical rotations were measured on a JASCO P-1000 automatic polarimeter. HPLC analyses were carried out with JASCO instruments (pump, PU-2080 plus; detector, UV-2075). The enantiomeric excess was determined by HPLC using Daicel Chiralcel OD-H (25 cm × 0.46 cm i.d.) column. Fluorescence and UV–vis absorption spectra were measured on a JASCO FP-8300 fluorescence spectrometer. For the measurement of UV–vis absorption spectra in CH_3CN, an FUV-803 absorbance measurement cell block was used. Circular dichroism (CD) spectra were recorded on a JASCO J-725 spectrometer. Melting points were determined on a Stuart melting point apparatus SMP3 and are uncorrected. High-resolution electrospray ionization (HRMS-ESI) mass spectra were recorded on a Hitachi Nano Frontier LD spectrometer. Silica gel 60 N (spherical, neutral, 63–210 μm) was used for column chromatography. Diethylene glycol bis(*p*-toluenesulfonate),[49] (2-((3*R*,7a*S*)-2-phenylhexahydro-1*H*-pyrrolo[1,2-*c*]imidazol-3-yl)phenyl)bis(3-(trifluoromethyl)phenyl)methanol (**4**),[40] and 1,1′-bipyrene (**6**)[47] were synthesized according to the literature procedures. A hexane solution of diethylzinc (1.1 M, Kanto Chemical Co., Inc., Japan) was used for the enantioselective addition. The spectroscopic-grade solvents for UV–vis absorption, CD, and fluorescence measurements were purchased from FUJIFILM Wako Pure Chemical Corporation and used as received. Perchlorates were purchased from FUJIFILM Wako Pure Chemical Corporation, Kanto Chemical Co., Inc., and Nacalai Tesque, Inc.

Synthesis of (*S*,*S*)-1, (*R*,*R*)-1, (*S*)-2, (*S*)-5, and (*R*)-5

(*S*,*S*)-Diethylene glycol bis[1-(1-pyren-1-yl)propyl]ether (1)

A mixture of NaH (0.434 g, 9.95 mmol, 55% in oil) and (*S*)-1-(pyren-1-yl)propan-1-ol (**5**) (0.571 g, 2.19 mmol) in *N*,*N*-dimethylformamide (17.0 mL) was stirred at 70 °C for 1 h. To the mixture was added a *N*,*N*-dimethylformamide (12.0 mL) solution of diethylene glycol ditosylate (0.405 g, 1.00 mmol) and

the mixture was stirred at room temperature for 24 h. Saturated aqueous ammonium chloride solution was added to the reaction mixture. The aqueous layer was separated and extracted with hexane/AcOEt (4:1) three times. The combined organic layer was washed with water and brine, dried over anhydrous Na_2SO_4, and filtered. After removal of the solvent under reduced pressure, the crude product was purified by column chromatography on silica gel (hexane/AcOEt = 4:1) to give (*S*,*S*)-**1** (0.345 g, 59%) as a yellow solid. M.p.: 44.4–45.0 °C; $[\alpha]_D^{20}$ –46.6 (*c* 1.0, $CHCl_3$); IR (KBr): ν_{max} 3040, 2962, 2929, 2871, 1602, 1586, 1458, 1111, 1089, 847 cm^{-1}; ^1H NMR (500 MHz, $CDCl_3$): δ (ppm) 8.39 (d, *J* = 9.5 Hz, 2H), 8.17–8.08 (m, 8H), 8.05–7.96 (m, 8H), 5.24 (t, *J* =6.8 Hz, 2H), 3.67–3.61 (m, 4H), 3.54 (t, *J* = 4.9 Hz, 4H), 2.11–1.95 (m, 4H), 0.98 (t, *J* = 7.4 Hz, 6H); ^{13}C NMR (126 MHz, $CDCl_3$): δ (ppm) 136.3, 131.3, 130.7, 130.5, 128.5, 127.5, 127.3, 127.0, 125.8, 125.1, 124.93, 124.89, 124.85, 124.6, 122.8, 81.6, 70.7, 68.4, 31.3, 10.7 (one signal is hidden by incidental overlapping); HRMS-ESI (*m*/*z*): $[M+Na]^+$ calcd for $C_{42}H_{38}O_3Na$, 613.2713; found, 613.2739.

(*R*,*R*)-Diethylene glycol bis[1-(1-pyren-1-yl)propyl]ether (1)

According to the same experimental procedure as the synthesis of (*S*,*S*)-**1**, the mixture of (*R*)-**5** (0.577 g, 2.22 mmol) and diethylene glycol ditosylate (0.408 g, 1.00 mmol) in the presence of NaH (0.436 g, 10.0 mmol, 55% in oil) was stirred at 70 °C in *N*,*N*-dimethylformamide (29.0 mL) for 24 h to give (*R*,*R*)-**1** (0.372 g, 63%) as a yellow solid. $[\alpha]_D^{20}$ +42.9 (*c* 1.0, $CHCl_3$).

(*S*)-1-[1-(2-Ethoxyethoxy)propyl]pyrene (2)

According to the same experimental procedure as the synthesis of (*S*,*S*)-**1**, the mixture of (*S*)-**5** (0.519 g, 1.99 mmol) and 2-bromoethyl ethyl ether (1.53 g, 10.0 mmol) in the presence of NaH (0.432 g, 9.91 mmol, 55% in oil) was stirred at room temperature in *N*,*N*-dimethylformamide (14.5 mL) for 24 h to give (*S*)-**2** (0.464 g, 70%) as a yellow oil. $[\alpha]_D^{25}$ –63.8 (*c* 1.0, $CHCl_3$); IR (KBr): ν_{max} 3041, 2972, 2929, 2869, 1601, 1587, 1457, 1113, 848, 718 cm^{-1}; ^1H NMR (500 MHz, $CDCl_3$): δ (ppm) 8.44 (d, *J* = 9.5 Hz, 1H), 8.19 (d, *J* = 7.5 Hz, 1H), 8.17 (d, *J* = 7.5 Hz, 2H), 8.12 (d, *J* = 7.5 Hz, 1H), 8.09 (d, *J* = 9.5 Hz, 1H), 8.05 (s, 2H), 7.99 (t, *J* = 7.5 Hz 1H), 5.27 (t, *J* = 6.6 Hz, 2H), 3.64–3.58 (m, 2H), 3.57–3.46 (m, 4H), 2.17–2.09 (m, 1H), 2.06–1.97 (m, 1H), 1.20 (t, *J* = 6.9 Hz, 3H), 1.00 (t, *J* = 7.4 Hz, 3H); ^{13}C NMR (126 MHz, $CDCl_3$): δ (ppm) 136.3, 131.4, 130.7, 130.5, 128.5, 127.5, 127.3, 127.1, 125.8, 125.1, 124.94, 124.86, 124.6, 122.9, 81.7, 70.0, 68.4, 66.5, 31.3, 15.2, 10.8; HRMS-ESI (m/z): $[M]^+$ calcd for $C_{23}H_{24}O_2$, 332.1771; found, 322.1768.

(*S*)-1-(Pyren-1-yl)propan-1-ol (5)[50]

To a stirred solution of 1,4-amino alcohol (3*R*,7a*S*)-**4** (0.583 g, 1.00 mmol) in toluene (15.0 mL), a hexane solution (1.1 M) of diethylzinc (18.4 mL, 20.0 mmol) was added dropwise through a syringe at 0 °C. The reaction mixture was stirred at room temperature for 30 min. To the mixture was added dropwise a toluene/CH_2Cl_2 solution (3:1, 20.0 mL) of 1-pyrenecarbaldehyde (**3**: 2.29 g, 9.9 mmol) and the mixture was stirred at room temperature for 18 h. Saturated aqueous ammonium chloride solution and 2M aqueous HCl were added to the reaction mixture. The aqueous layer was separated and extracted with CH_2Cl_2 three times. The combined organic layer was washed with water and brine, dried over anhydrous Na_2SO_4, and filtered. After removal of the solvent under reduced pressure, the crude product was purified by column chromatography on silica gel (toluene/CH_2Cl_2=1:1) followed by single recrystallization from cyclohexane to give (*S*)-**5** (1.74 g, 67%, >99% ee) as a white solid.

The enantiomeric excess of (*S*)-**5** was determined to be >99% by HPLC analysis using a chiral column [Chiralcel OD-H; 254 nm UV detector; eluent, hexane/*i*-PrOH = 90:10; flow rate, 0.5 mL/min; *t*, 24.2 min for (*S*)-**5**, 28.0 min for (*R*)-**5**]. The retention time of (*R*)-**5** was determined by using *rac*-**5** prepared by the reaction of ethylmagnesium bromide with 1-pyrenecarbaldehyde.

(*R*)-1-(Pyren-1-yl)propan-1-ol (5)

According to the same experimental procedure as the synthesis of (*S*)-**1**, the mixture of **3** (2.30 g, 9.99 mmol) and a hexane solution (1.1 M) of diethylzinc (18.4 mL, 20.0 mmol) in the presence of (3*S*,7a*R*)-**4** (0.582 g, 1.00 mmol) was stirred at room temperature in a toluene/CH_2Cl_2 solution (6:1, 35.0 mL) for 18 h to give (*R*)-**5** (1.30 g, 50%, >99% ee) after single recrystallization from cyclohexane.

Typical experimental procedure for the cation recognition experiments

A 2.5 mM CH_3CN solution of (*S*,*S*)-**1** (solution A) was prepared in a 10 mL volumetric flask by dissolving (*S*,*S*)-**1** (14.8 mg, 0.025 mmol) into CH_3CN. A 25 mM CH_3CN solution of perchlorate salts (solution B) was prepared in a 5 mL volumetric flask by dissolving $Al(ClO_4)_3 \bullet 9H_2O$ (61.0 mg, 0.125 mmol) into CH_3CN. A 1.0×10^{-5} M CH_3CN solution of (*S*,*S*)-**1** (solution C) was prepared in a 5 mL volumetric flask by dilution of solution A (20 μL) with CH_3CN. A 1.0×10^{-5} M CH_3CN solution of (*S*,*S*)-**1** with 10 or 100 equivalents of perchlorate salts (solutions D and E) was prepared in a 5 mL volumetric flask by dilution of solution A (20 μL) and solution B (100 μL or 1000 μL) with CH_3CN.

Typical experimental procedure for the determination of association constants by fluorescence titration

Sample preparation. A 2.5 mM CH_3CN solution of (*S*,*S*)-**1** (solution A) was prepared in a 10 mL volumetric flask by dissolving (*S*,*S*)-**1** (14.8 mg, 0.025 mmol) into CH_3CN. A 25 mM CH_3CN solution of $Al(ClO_4)_3 \bullet 9H_2O$ (solution B) was prepared in a 5 mL volumetric flask by dissolving $Al(ClO_4)_3 \bullet 9H_2O$ (61.0 mg, 0.125 mmol) into CH_3CN. A 5.0×10^{-6} M CH_3CN solution of (*S*,*S*)-**1** (solution C) was prepared in a 5 mL volumetric flask by dilution of solution A (10 μL) with CH_3CN. A 5.0×10^{-5} M, 5.0×10^{-4} M, or 5.0×10^{-3} M CH_3CN solution of $Al(ClO_4)_3 \bullet 9H_2O$ containing 5.0×10^{-6} M of (*S*,*S*)-**1** (solutions D, E, and F) was prepared in a 5 mL volumetric flask by dilution of solution A (10 μL) and solution B (10 μL, 100 μL, or 1000 μL) with CH_3CN.

Titration protocol. Initially, the fluorescence spectrum of solution C (2.0 mL) in a 10 mm quartz cell was recorded at 25 °C. To solution C were added small aliquots of solution D (20 μL, 21

μL × 3, 22 μL, 23 μL × 3, 24 μL, 25 μL, 63 μL, and 68 μL), solution E (12 μL, 24 μL, 25 μL, 26 μL × 3, 28 μL, 27 μL, and 29 μL) and solution F (26 μL, 27 μL, 28 μL × 2, and 149 μL). After each aliquot addition, the fluorescence spectrum in the range between 350 and 700 nm was recorded. Each titration experiment was carried out three times. The association constants (K_a) were determined using the BindFit calculator.[51–53] In all cases, the simultaneous fitting analysis of the experimental data yielded the most reliable results for a simple 1:1 binding model.

Conflicts of interest

There are no conflicts to declare.

Acknowledgements

This work was partly supported by JSPS KAKENHI Grant Number JP20K05645 within a Grant-in-Aid for Scientific Research (C) and Yokohamakogyokai research foundation.

Notes and references

1 M. H. Chua, H. Zhou, Q. Zhu, B. Z. Tang and J. W. Xu, *Mater. Chem. Front*., 2021, **5**, 659–708.
2 J. Yin, Y. Hu and J. Yoon, *Chem. Soc. Rev.*, 2015, **44**, 4619–4644.
3 Y. Jeong and J. Yoon, *Inorg. Chim. Acta*, 2012, **381**, 2–14.
4 K. Rurack, *Spectrochim. Acta, Part A*, 2001, **57**, 2161–2195.
5 B. Valeur and I. Leray, *Coord. Chem. Rev.*, 2000, **205**, 3–40.
6 E. Manandhar and K. J. Wallace, *Inorg. Chim. Acta*, 2012, **381**, 15–43.
7 S. Karuppannan and J.-C. Chambron, *Chem. - Asian J.*, 2011, **6**, 964–984.
8 X. Chen, T. Pradhan, F. Wang, J. S. Kim and J. Yoon, *Chem. Rev.*, 2012, **112**, 1910–1956.
9 E. M. Nolan and S. J. Lippard, *J. Am. Chem. Soc.*, 2003, **125**, 14270–14271.
10 S. C. Burdette, G. K. Walkup, B. Spingler, R. Y. Tsien and S. J. Lippard, *J. Am. Chem. Soc.*, 2001, **123**, 7831–7841.
11 D. Cao, Z. Liu, P. Verwilst, S. Koo, P. Jangjili, J. S. Kim and W. Lin, *Chem. Rev.*, 2019, **119**, 10403–10519.
12 K. C. Ko, J.-S. Wu, H. J. Kim, P. S. Kwon, J. W. Kim, R. A. Bartsch, J. Y. Lee and J. S. Kim, *Chem. Commun*., 2011, **47**, 3165–3167.
13 H. S. Jung, P. S. Kwon, J. W. Lee, J. I. Kim, C. S. Hong, J. W. Kim, S. Yan, J. Y. Lee, J. H. Lee, T. Joo and J. S. Kim, *J. Am. Chem. Soc.*, 2009, **131**, 2008–2012.
14 E. V. Antina, N. A. Bumagina, A. I. V'yugin and A. V. Solomonov, *Dyes Pigm.*, 2017, **136**, 368–381.
15 X. Peng, J. Du, J. Fan, J. Wang, Y. Wu, J. Zhao, S. Sun and T. Xu, *J. Am. Chem. Soc.*, 2007, **129**, 1500–1501.
16 L. Zeng, E. W. Miller, A. Pralle, E. Y. Isacoff and C. J. Chang, *J. Am. Chem. Soc.*, 2006, **128**, 10–11.
17 K. Fujimoto, Y. Muto and M. Inouye, *Chem. Commun*., 2005, 4780–4782.
18 A. Dhir, V. Bhalla and M. Kumar, *Tetrahedron Lett*., 2008, **49**, 4227–4230.
19 H. J. Kim, S. H. Kim, D. T. Quang, J. H. Kim, I.-H. Suh and J. S. Kim, *Bull. Korean Chem. Soc.*, 2007, **28**, 811–815.
20 E. J. Jun, H. N. Won, J. S. Kim, K.-H. Lee and J. Yoon, *Tetrahedron Lett.*, 2006, **47**, 4577–4580.
21 S. K. Kim, S. H. Lee, J. Y. Lee, J. Y. Lee, R. A. Bartsch and J. S. Kim, *J. Am. Chem. Soc.*, 2004, **126**, 16499–16506.
22 J.-S. Yang, C.-S. Lin and C.-Y. Hwang, *Org. Lett.*, 2001, **3**, 889–892.
23 R. Kumar, V. Bhalla and M. Kumar, *Tetrahedron*, 2008, **64**, 8095–8101.
24 J. Xie, M. Ménand, S. Maisonneuve and R. Métivier, *J. Org. Chem.*, 2007, **72**, 5980–5985.
25 J. S. Kim, M. G. Choi, K. C. Song, K. T. No, S. Ahn and S.-K. Chang, *Org. Lett.*, 2007, **9**, 1129–1132.
26 J. Y. Lee, S. K. Kim, J. H. Jung and J. S. Kim, *J. Org. Chem.*, 2005, **70**, 1463–1466.
27 C. Kar, M. D. Adhikari, A. Ramesh and G. Das, *RSC Adv.*, 2012, **2**, 9201–9206.
28 H. S. Jung, M. Park, D. Y. Han, E. Kim, C. Lee, S. Ham and J. S. Kim, *Org. Lett.*, 2009, **11**, 3378–3381.
29 S.-Y. Moon, N. J. Youn, S. M. Park and S.-K. Chang, *J. Org. Chem.*, 2005, **70**, 2394–2397.
30 H. Yuasa, N. Miyagawa, T. Izumi, M. Nakatani, M. Izumi and H. Hashimoto, *Org. Lett.*, 2004, **6**, 1489–1492.
31 X.-J. Jiang and D. K. P. Ng, *Angew. Chem., Int. Ed.*, 2014, **53**, 10481–10484.
32 D. Maity and T. Govindaraju, *Chem. Commun.*, 2012, **48**, 1039–1041.
33 J. F. Zhang, Y. Zhou, J. Yoon, Y. Kim, S. J. Kim and J. S. Kim, *Org. Lett.*, 2010, **12**, 3852–3855.
34 L. Xue, Q. Liu and H. Jiang, *Org. Lett.*, 2009, **11**, 3454–3457.
35 Z. Guo, W. Zhu, L. Shen and H. Tian, *Angew. Chem., Int. Ed.*, 2007, **46**, 5549–5553.
36 H. Komatsu, T. Miki, D. Citterio, T. Kubota, Y. Shindo, Y. Kitamura, K. Oka and K. Suzuki, *J. Am. Chem. Soc.*, 2005, **127**, 10798–10799.
37 X. Liu, X. Yang, Y. Fu, C. Zhu and Y. Cheng, *Tetrahedron*, 2011, **67**, 3181–3186.
38 J. K. Choi, S. H. Kim, J. Yoon, K.-H. Lee, R. A. Bartsch and J. S. Kim, *J. Org. Chem.*, 2006, **71**, 8011–8015.
39 S. H. Kim, J. S. Kim, S. M. Park and S.-K. Chang, *Org. Lett.*, 2006, **8**, 371–374.
40 V. A. Nefedov, *Russ. J. Org. Chem.*, 2007, **43**, 1163–1166.
41 M. Asami, A. Hasome, N. Yachi, N. Hosoda, Y. Yamaguchi and S. Ito, *Tetrahedron: Asymmetry*, 2016, **27**, 322–399.
42 S. Ito, K. Ikeda and M. Asami, *Chem. Lett.*, 2016, **45**, 1379–1381.
43 S. Ito, M. Okuno and M. Asami, *Org. Biomol. Chem.*, 2018, **16**, 213–222.
44 S. Ito, S. Okada, R. Sue and M. Asami, *Chem. Lett.*, 2018, **47**, 340–343.
45 S. Ito, K. Ikeda, S. Nakanishi, Y. Imai and M. Asami, *Chem. Commun.*, 2017, **53**, 6323–6326.
46 S. Ito, R. Sekine, M. Munakata, M. Asami, T. Tachikawa, D. Kaji, K. Mishima and Y. Imai, *ChemPhotoChem*, 2021, **5**, 920–925.
47 T. Yoshinaga, H. Hiratsuka and Y. Tanizaki, *Bull. Chem. Soc. Jpn.*, 1977, **50**, 3096–3102.
48 M. Yamaji, H. Okamoto, K. Goto, F. Tani, *J. Photochem. Photobiol., A*, 2021, **421**, 113518.
49 E. Bednářová, S. Hybelbauerová and J. Jindřich, *Beilstein J. Org. Chem.* 2016, **12**, 349–352.
50 W.-K. An, M.-Y. Han, C.-A. Wang, S.-M. Yu, Y. Zhang, S. Bai and W. Wang, *Chem. - Eur. J.*, 2014, **20**, 11019–11028.
51 Bindfit. http://app.supramolecular.org/bindfit/, accessed Jan 5, 2022.
52 P. Thordarson, *Chem. Soc. Rev.*, 2011, **40**, 1305−1323.
53 D. B. Hibbert and P. Thordarson, *Chem. Commun.*, 2016, **52**, 12792–12805.